Environment International 156 (2021) 106718

Contents lists available at ScienceDirect

Environment International

journal homepage: www.elsevier.com/locate/envint

In vitro hazard characterization of simulated aircraft cabin bleed-air contamination in lung models using an air-liquid interface (ALI) exposure system

Rui-Wen He [a,b], Marc M.G. Houtzager [c], W.P. Jongeneel [a], Remco H.S. Westerink [b], Flemming R. Cassee [a,b,*]

[a] National Institute for Public Health and the Environment (RIVM), P.O. Box 1, 3720 BA Bilthoven, the Netherlands
[b] Institute for Risk Assessment Sciences (IRAS), Toxicology Division, Faculty of Veterinary Medicine, Utrecht University, P.O. Box 80177, 3508 TD Utrecht, the Netherlands
[c] The Netherlands Organisation for Applied Scientific Research, TNO, P.O. Box 80015, 3508 TA Utrecht, the Netherlands

ARTICLE INFO

Handling Editor: Martí Nadal

Keywords:
Fume event
Aircraft cabin air
Mini-BACS
Organophosphates
Co-culture
BMD analysis

ABSTRACT

Contamination of aircraft cabin air can result from leakage of engine oils and hydraulic fluids into bleed air. This may cause adverse health effects in cabin crews and passengers. To realistically mimic inhalation exposure to aircraft cabin bleed-air contaminants, a mini bleed-air contaminants simulator (Mini-BACS) was constructed and connected to an air-liquid interface (ALI) aerosol exposure system (AES). This unique "Mini-BACS + AES" setup provides steady conditions to perform ALI exposure of the mono- and co-culture lung models to fumes from pyrolysis of aircraft engine oils and hydraulic fluids at respectively 200 °C and 350 °C. Meanwhile, physico-chemical characteristics of test atmospheres were continuously monitored during the entire ALI exposure, including chemical composition, particle number concentration (PNC) and particles size distribution (PSD). Additional off-line chemical characterization was also performed for the generated fume. We started with submerged exposure to fumes generated from 4 types of engine oil (Fume A, B, C, and D) and 2 types of hydraulic fluid (Fume E and F). Following submerged exposures, Fume E and F as well as Fume A and B exerted the highest toxicity, which were therefore further tested under ALI exposure conditions. ALI exposures reveal that these selected engine oil (0–100 mg/m^3) and hydraulic fluid (0–90 mg/m^3) fumes at tested dose-ranges can impair epithelial barrier functions, induce cytotoxicity, produce pro-inflammatory responses, and reduce cell viability. Hydraulic fluid fumes are more toxic than engine oil fumes on the mass concentration basis. This may be related to higher abundance of organophosphates (OPs, ≈2800 μg/m^3) and smaller particle size (≈50 nm) of hydraulic fluid fumes. Our results suggest that exposure to engine oil and hydraulic fluid fumes can induce considerable lung toxicity, clearly reflecting the potential health risks of contaminated aircraft cabin air.

1. Introduction

Concerns have been raised regarding the potential health risks of exposure to contaminated air in aircraft cabins (Michaelis, 2011; Ramsden, 2012; Winder and Michaelis, 2005). Health effects reported by a fraction of aircraft cabin crews include cough, sore throat, nausea, dizziness, disorientation, and tremors during flight. Those health complaints, which are sometimes collectively referred to as "aerotoxic syndrome" (Michaelis et al., 2017; Van Netten, 2005), have been associated with exposure to cabin air contaminants, particularly during so-called fume events (Abou-Donia et al., 2013; Brown et al., 2001; Reneman et al., 2016; Winder and Michaelis, 2005).

The primary source of outside air used to pressurize and ventilate the cabin and cockpit (so-called "bleed air") is extracted from the main engine compressors (during flight) or from the Auxiliary Power Unit (on ground level). Bleed air passes through the air conditioning system (so-called "PACKs") of the Environmental Control System (ECS) before being distributed to aircraft cabin and cockpit. However, during this process, bleed air contamination may occur, for example, due to oil leaks. Oils from those leaks are subjected to high temperatures and their

* Corresponding author at: National Institute for Public Health and the Environment (RIVM), P.O. Box 1, 3720 BA Bilthoven, the Netherlands.
E-mail address: flemming.cassee@rivm.nl (F.R. Cassee).

https://doi.org/10.1016/j.envint.2021.106718
Received 15 March 2021; Received in revised form 9 June 2021; Accepted 11 June 2021
Available online 21 June 2021

thermal degradation products can contaminate bleed air, subsequently resulting in aircraft cabin air contamination (Michaelis, 2011; Michaelis, 2016). It has been reported that organophosphates (OPs), volatile organic compounds (VOCs), carbon monoxide (CO) and ultrafine particles (UFPs, particle size <100 nm) are the main contaminants (Denola et al., 2011; Howard et al., 2018; Shehadi et al., 2016; Solbu et al., 2011).

Inhalation exposure to a complex mixture of those contaminants in an aircraft cabin may pose considerable health risks for crews and passengers (Michaelis et al., 2017). A large health survey on 4011 flight attendants, conducted by the Occupational Health Research Consortium in Aviation (OHRCA) in 2014, showed that almost 50% of flight attendants reported one or more symptoms, in which respiratory symptoms and neurological problems accounted for 23% and 17%, respectively (OHRCA, 2014). However, given the difficulties to capture fume events in real time in aircraft cabins, current information on characteristics of fume events as well as their inhalation toxicity is still scarce.

The use of a simulation setup for generating fumes under controlled laboratory conditions allows a steady output of test atmospheres to measure the composition (e.g. chemicals and particles) of fume events, regardless the type and state of the engine or ECS. It has been reported that various chemicals can be derived from simulated fume events, of which CO and tricresyl phosphate (TCP) isomers were the most frequently reported compounds (Van Netten and Leung, 2001; Winder and Balouet, 2002). High concentrations of UFPs were also detected after pyrolysis of aircraft engine oils (Amiri et al., 2017; Mann et al., 2014). The chemical composition of fume emissions from laboratory pyrolysis can differ depending on oil types (Van Netten and Leung, 2001), which probably affects toxic properties of the generated fumes. Therefore, understanding the composition profile of fumes generated from different types of aircraft engine oil and hydraulic fluid is essential for further investigation of inhalation toxicity by cabin air contaminants.

Upon inhalation, particles can be gradually deposited onto human tracheobronchial epithelium based on the size and aerodynamic behaviour (Braakhuis et al., 2014). Therefore, human bronchial epithelial cell models are preferred for inhalation exposure studies. To more accurately evaluate the responses to UFPs originating from, for example, pyrolyzed oils, macrophages can be added onto the epithelial carpet (Ji et al., 2018; Wottrich et al., 2004), as macrophages are known to play an important role in the uptake and clearance of particles in the lungs (Hu and Christman, 2019). Importantly, cell models should allow for a continuous exposure to the generated fumes under air-liquid interface (ALI) exposure conditions to realistically mimic inhalation exposure of the bronchial epithelium.

The primary goal of this study is to investigate the hazards of simulated aircraft fume events under controlled laboratory conditions. We hypothesize that aircraft engine oil and hydraulic fluid fumes can induce cytotoxicity and inflammation responses in human lung cell models under ALI exposure conditions. To test this hypothesis, a mini bleed-air contaminants simulator (Mini-BACS) was set up for generating fumes, including 4 types of engine oil fumes (Fume A, B, C, and D) and 2 types of hydraulic fluid fumes (Fume E and F). Chemical composition, particle number concentration (PNC), and particles size distribution (PSD) of the generated fumes were investigated. For testing the toxicity of the generated fumes *in vitro*, we started with submerged exposure of the lung model to establish a dose-response relationship to gain a basic understanding of their toxic potency. In accordance with the results obtained from submerged exposure, the 4 types of fume samples that exerted the highest toxicity were selected and subsequently tested under ALI exposure conditions to further evaluate their toxicity. An aerosol exposure system (AES) was connected with the Mini-BACS to allow long-term ALI exposure to the generated fumes using a monoculture of human bronchial epithelial (Calu-3) cells and a co-culture of Calu-3 + human monocyte-derived macrophages (MDMs). Adverse effects on the cell models, including changes in transepithelial electrical resistance (TEER), cell viability, lactate dehydrogenase (LDH) release and inflammatory responses, were measured at 24 h post exposure. Additionally, the off-line chemical characterization was performed to measure the concentrations of aldehydes-ketones, OPs, VOCs, and organic acids in the generated aircraft cabin fumes.

2. Materials and methods

2.1. Chemicals and reagents

We selected 4 types of engine oil and 2 types of hydraulic fluid that are the most abundant based on market share. More information of those samples, provided by distributors of aviation oils and fluids, is shown in Table S1. Culture medium and supplements, as well as enzyme-linked immunosorbent assay (ELISA) kits for measuring interleukin (IL)-6, IL-8, IL-10 and tumor necrosis factor (TNF)-α were purchased from Life Technologies (Thermo Fisher Scientific Inc., the Netherlands); WST assay kit was purchased from Promega (Fitchburg, Wisconsin, USA); LDH detection kit was purchased from Roche Diagnostics (Mannheim, Germany); All other chemicals, unless otherwise noted, were purchased from Sigma Aldrich (the Netherlands).

2.2. Cell culture under submerged and ALI conditions

Calu-3 cells purchased from American Tissue Culture Collection (ATCC, Rockville, MD) were cultured in minimum essential medium (MEM) with 10% fetal bovine serum (FBS), 1% Non-Essential Amino Acid (NEAA) solution and 1% penicillin/streptomycin. Primary human $CD14^+$ monocytes isolated from buffy coats (Sanquin, the Netherlands) were differentiated to MDMs by addition of macrophage colony-stimulating factor (M-CSF, 50 ng/mL) for 6 days as previously described (He et al., 2021). Monocytes and macrophages were cultured in RPMI-1640 medium with 10% FBS and 1% penicillin/streptomycin. All cells were cultured in flasks in an incubator with 5% CO_2 at 37 °C.

When reaching approximately 80% confluence, Calu-3 cells were detached enzymatically by 0.05% trypsin-EDTA. Then, 0.5 mL of cell suspension (density: 2.5×10^5 cells/mL) was seeded on the apical side of cell culture inserts (0.4 μm pore membrane, 1.12 cm^2 polyester membrane, Costar, Germany) in 12-well plates, with 1.5 mL cell culture medium on the basolateral side of the inserts for nutrient supply. After submerged culture for 7 days to reach confluence, the apical medium was removed to obtain ALI conditions. Calu-3 cells on the inserts were cultured for an additional 7 days under ALI conditions before being used for subsequent ALI exposure or co-culture with MDMs. To create the Calu-3 + MDM co-culture model, 0.5 mL of MDMs suspension was added onto the Calu-3 epithelial carpet for 4 h with a density of 5×10^4 macrophages/cm^2. After removing the apical medium, the Calu-3 + MDM co-culture model was cultured for an additional 20 h under ALI conditions. During cell culture on the inserts, the apical and basolateral medium were refreshed every 2 or 3 days.

2.3. Mini-BACS setup

As illustrated in Fig. 1, aircraft engine oil and hydraulic fluid samples were guided to a spray nozzle (Schlick, Germany) by an adjustable motor driven syringe to be nebulized with pre-heated (90 °C) air into a heated mixing chamber (90 °C), controlled by a mass flow controller (MFC). The fumes then flowed through an oven (R50/500/12, Nabertherm, Germany) for pyrolysis and vaporization. In previous studies, pyrolysis experiments were performed at various temperatures in the range from 200 to 600 °C (Amiri et al., 2017; Mann et al., 2014; Van Netten and Leung, 2001). Different temperatures will most likely have an effect on aerosol characteristics, however, according to the report of National Research Council (NRC) (2002), typical conditions for bleed air of an aircraft engine do not exceed 350 °C (NRC, 2002). To realistically reflect conditions during fume events, we therefore used 350 °C and

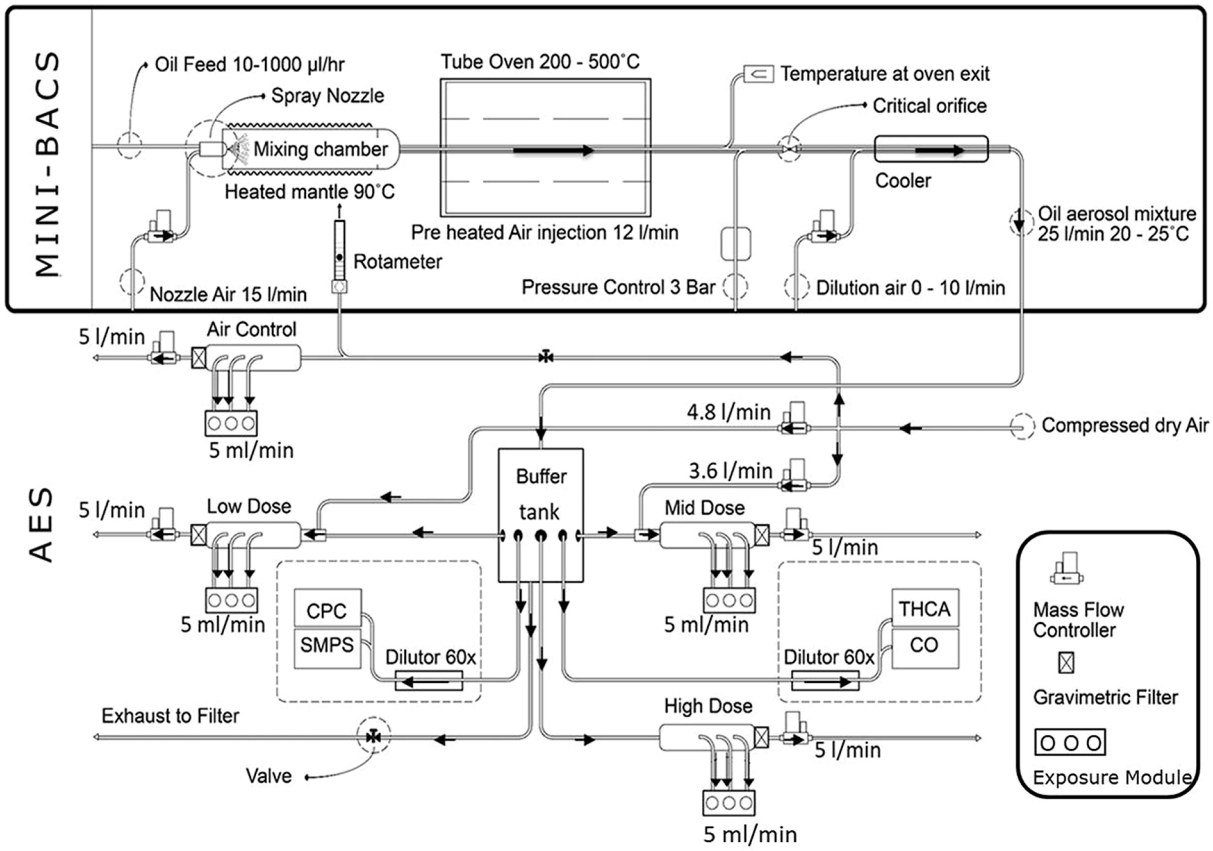

Fig. 1. Schematic representation of the mini bleed-air contaminants simulator (Mini-BACS, top) and ALI aerosol exposure system (AES, bottom). The Mini-BACS is connected to the AES for exposure to the generated fumes *in vitro*. The AES contains 4 exposure modules including 1 module for exposure to clean air (air control) and 3 for exposure to the generated fumes at 3 doses each. For online measurement of particle number concentration (PNC), particle size distribution (PSD), and concentrations of volatile organic compounds (VOCs) and CO, the AES is connected to a condensation particle counter (CPC), a scanning mobility particle sizer (SMPS), a total hydrocarbon analyzer (THCA) and a gas filter correlation carbon monoxide (CO) analyzer.

200 °C as the pyrolysis temperature for aircraft engine oils and hydraulic fluids, respectively. The whole system was kept pressurized at around 3 bar using a critical orifice downstream of the oven and a back pressure regulator. After expanding through the critical orifice to atmospheric pressure, the generated fumes were diluted and cooled with compressed air controlled by a MFC to 20–25 °C measured by a temperature sensor, and transferred to a buffer tank made of anodized aluminum. To continuously monitor the characteristics of test atmospheres in the buffer tank, including PNC, PSD, and concentrations of VOCs and CO, we used a condensation particle counter (CPC) 3752 (TSI inc., St Paul MN, USA), a scanning mobility particle sizer (SMPS) 3936 (TSI inc., St Paul MN, USA), a total hydrocarbon analyser (THCA) RS 55-T (Ratfisch Analysensysteme GmbH., Poing, Germany) and a gas filter correlation CO analyser model 300E (ENVIRO-TEC., Largo Lakes Blvd, USA).

2.4. Fume sampling, chemical analysis and submerged exposure

Fumes generated from aircraft engine oil and hydraulic fluid with the Mini-BACS were collected for chemical analysis and *in vitro* toxicity testing via submerged exposure. Concentrations of aldehydes-ketones (C1 - C6), OPs (32 OPs), VOCs (C6 - C12), and organic acids (C1 - C8) in collected fume samples were measured. Details of sampling, extraction and chemical analysis can be found in the Supplementary Material.

To perform submerged exposure, Calu-3 cell suspension (density: 8 × 10^5 cells/mL) was added into 96-well plates (100 µL per well) and cells were cultured for 24 h to reach confluence. Before submerged exposure in 96-well plates, fume extracts in vials (described in the Supplementary Material) were dissolved in pure DMSO to make stock solutions at 100 mg/mL. The solution of each fume sample was subsequently diluted in Calu-3 cell culture medium to 8 exposure doses ranging from 4 to 512 µg/mL containing 0.5% DMSO. Calu-3 cells were exposed to those samples at 8 doses in triplicate for 24 h. The medium suspension of blank filter extracts containing 0.5% DMSO and the fresh culture medium were used as negative controls and medium controls, respectively.

2.5. ALI exposure to the generated fumes

The AES (Vitrocell, Waldkirch, Germany) used for this study has 4 exposure modules, including 1 module for exposure to clean air and 3 for exposure to the generated fumes at different doses (Fig. 1 and Figure S1). Before starting an exposure, we filled each well in the modules with 3.5 mL of Calu-3 cell culture medium and then transferred the inserts with the cells to each well. From the buffer tank (described in 2.3), streams of the generated fumes were fed into three manifolds where fumes were diluted with compressed air. A small volume of fume taken from each manifold was sprayed via the AES, with a flow-rate at 5 mL/min, onto the cells on the inserts for 4 h at 37 °C and 85% humidity. Compressed clean air with the same flow-rate was used as clean air control. The main flow of fume or compressed air through each manifold (5 L/min) was collected on filters (PTFE Membrane Disc Filters – 2 µm, VWR, the Netherlands) for calculating their mass concentrations during exposure:

$$\text{Mass concentration}(\text{mg}/\text{m}^3) = \frac{\text{Fume mass on the filter (mg)} \times 1000}{5\ \text{L/min} \times 240\ \text{min}}$$

Notably, nucleation may occur when the emission of the oil vapor cools down to reach temperatures that also are present in aircraft cabins.

In our study, particle agglomeration may mostly occur between the generation of oil fumes (after cooling down) and deposition onto the cells. This gives a very short residence time of the generated fumes (<2 s) during this process, thus reducing chance of particle agglomeration. Meanwhile, 4 inserts were placed in an incubator: 3 for incubator controls and 1 for measuring the maximum LDH release (LDH_{max}) in the cells. After exposure in the AES for 4 h, the inserts with the cells were placed back to new 12-well plates with 1.5 mL culture medium on the basolateral side and transferred to an incubator for an additional 24-hour exposure.

2.6. Biological responses after submerged and ALI exposures

After submerged exposure to fume samples collected from pyrolysis of aircraft engine oils and hydraulic fluids for 24 h, viability of Calu-3 cells was measured via the WST assay as previously described (He et al., 2018) to establish the dose-response relationship for engine oil and hydraulic fluid samples.

TEER values of the Calu-3 monoculture and the Calu-3 + MDMs co-culture on the inserts were measured after exposure under ALI conditions for 24 h as an important indicator of barrier function and integrity in the lung cell models. The Evom2 Voltohmmeter with 4 mm chopstick electrodes (World Precision Instruments Inc., FL, USA) was used for TEER measurement by adding 0.5 mL culture medium to the apical side of the inserts. TEER values were corrected for the insert surface area (1.12 cm^2) and for the resistance of cell-free 12-well inserts (≈130 Ohm). After measuring TEER, apical and basolateral medium were collected and viabilities of the cells on the inserts were measured using the WST assay. Briefly, cells on the inserts were incubated with 10% WST solution for 30 min before absorbance measurement was performed as previously described (He et al., 2020). To investigate cytotoxicity, LDH release in the apical and basolateral medium was measured. Briefly, 100 μL of medium and 100 μL of LDH reagent were successively added to a 96-well plate and then incubated at room temperature (in dark) for 20 min before absorbance measurement. LDH values were corrected for the maximum LDH release (LDH_{max}) as previously described (He et al., 2020). In addition, production of cytokine IL-6, IL-8, IL-10 and TNF-α as markers for inflammatory responses in medium was measured using ELISA kits according to the manufacturer's protocol.

2.7. Statistical analysis

Results from submerged exposures were obtained from 2 independent experiments for each fume type, with 3 parallel inserts per experiment. Results from ALI exposures were obtained from 1 or 2 independent experiments for each fume type, with 3 or 4 parallel inserts per experiment. Differences between groups were compared by one-way analysis of variance (ANOVA), a p-value ≤ 0.05 is considered statistically significant. Data analysis was conducted using GraphPad software (version 8.2.1). Benchmark dose (BMD) analysis was used to derive a dose–response relationship for each fume sample (PROAST, version 67.0, www.rivm.nl/proast). More information of BMD analysis was described in our earlier study (He et al., 2020). In accordance with the European Food Safety Authority (EFSA) as well as taking the variation of the data into account, a 20% increase compared to incubator controls in total levels (apical + basolateral) of LDH release and inflammatory cytokines production was chosen as a benchmark response (BMR) for modelling (EFSA, 2009). After fitting the data to several models, the Exponential model turned out to be the optimal model for analysis. The lower 5% (BMDL) and upper 95% (BMDU) confidence limits (90% BMD confidence interval (BMDc.i.)) and the mean BMD of each fume were derived from the model analysis for effect markers. BMDc.i. was used for potency comparison between fume samples. More overlap between the BMDc.i of fume samples indicates less difference in their potency. If there was no 20% change or no BDMU determined at the tested dose-range, fume sample was not included in the rank order.

3. Results

3.1. Chemical profiles of fume samples

The concentration (μg/m^3) of aldehydes-ketones (C1 - C6), OPs (32 OPs), VOCs (C6 - C12), and organic acids (C1 - C8) in the collected fume samples were measured and total levels of aldehydes-ketones, OPs, VOCs, and organic acids were calculated (Fig. 2A and Table S2). Overall, engine oil fumes (Fume A, B, C and D) showed different concentration profiles. Total level of aldehydes-ketones was comparable among Fume A, B and D, around 6000 μg/m^3, which was higher than that of Fume C at 4257 μg/m^3. Fume B and C had a comparable OP level (≈2400 μg/m^3), which was around 2 and 5 times as high as that of Fume D (1077 μg/m^3) and Fume A (495 μg/m^3), respectively. Fume D had the highest level of organic acids (1246 μg/m^3), followed by Fume B (825 μg/m^3), Fume A (709 μg/m^3), and Fume C (340 μg/m^3). Total VOCs levels of engine oil fumes were relatively low ranging from 93 to 378 μg/m^3. In comparison to engine oil fumes, hydraulic fluid fumes had much lower levels of aldehydes-ketones (<80 μg/m^3) and organic acids (<10 μg/m^3), but relatively high levels of OP (≈2800 μg/m^3). The two hydraulic fluid fumes showed a comparable chemical profile, with the exception of total VOCs level which was around 60 times higher measured in Fume E (≈600 μg/m^3) compared to Fume F (≈10 μg/m^3).

3.2. Cell viability after submerged exposure

For viability of Calu-3 cells under submerged exposure conditions, a clear dose-response relationship was observed for all of fume samples at doses > 32 μg/mL (Fig. 2B). The median lethal concentration (LC_{50}) of fume samples for Calu-3 cells was calculated to rank their potency. Fume E and F had relatively low LC_{50} at 80 and 100 μg/mL, respectively, followed by Fume A and B at around 250 μg/mL, and Fume C and D at around 480 μg/mL. This indicates the higher toxicity of Fume E and F (hydraulic fluid fumes) as well as Fume A and B (engine oil fumes), which were therefore selected for subsequent ALI exposure using the Calu-3 monoculture cell model. Fume F was also tested using the Calu-3 + MDM co-culture model.

3.3. Characteristics of test atmospheres during ALI exposure

ALI exposure experiments were performed to more closely mimic inhalation exposure during a fume event. For ALI exposure, aircraft engine oils and hydraulic fluids were pyrolyzed at stable temperatures around 350 °C and 200 °C, respectively. In parallel, the characteristics of test atmospheres, including PNC, PSD and concentration of VOCs and CO, were continuously monitored during ALI exposure (Fig. 3 and Table 1). The geometric mean (GM) mobility diameter of engine oil fumes (≈100 nm) was twice as large as that of hydraulic fluid fumes (≈50 nm). The mean PNC of engine oil fumes was around 2.0×10^8/cm^3, which was higher than that of hydraulic fluid fumes (≈8.5×10^7/cm^3). The mean concentrations of VOCs and CO measured in engine oil fumes were around 10 and 20 ppm, respectively, which were higher than VOCs and CO levels of hydraulic fluid fumes (≈5.5 and 0.7 ppm, respectively). Mass concentrations of the generated fumes during ALI exposure were also calculated (Table 1). The highest exposure concentration was 100 mg/m^3 for Fume A and B, 55 mg/m^3 for Fume E, 90 mg/m^3 for Fume F with the Calu-3 monoculture, and 50 mg/m^3 Fume F with the Calu-3 + MDM co-culture.

3.4. Barrier functions and cell viability after ALI exposure

We measured TEER values and viabilities of the cells after ALI exposure to the different fumes for 24 h (Fig. 4). Compared to TEER values of controls, Calu-3 cells showed comparable TEER levels (≈1000

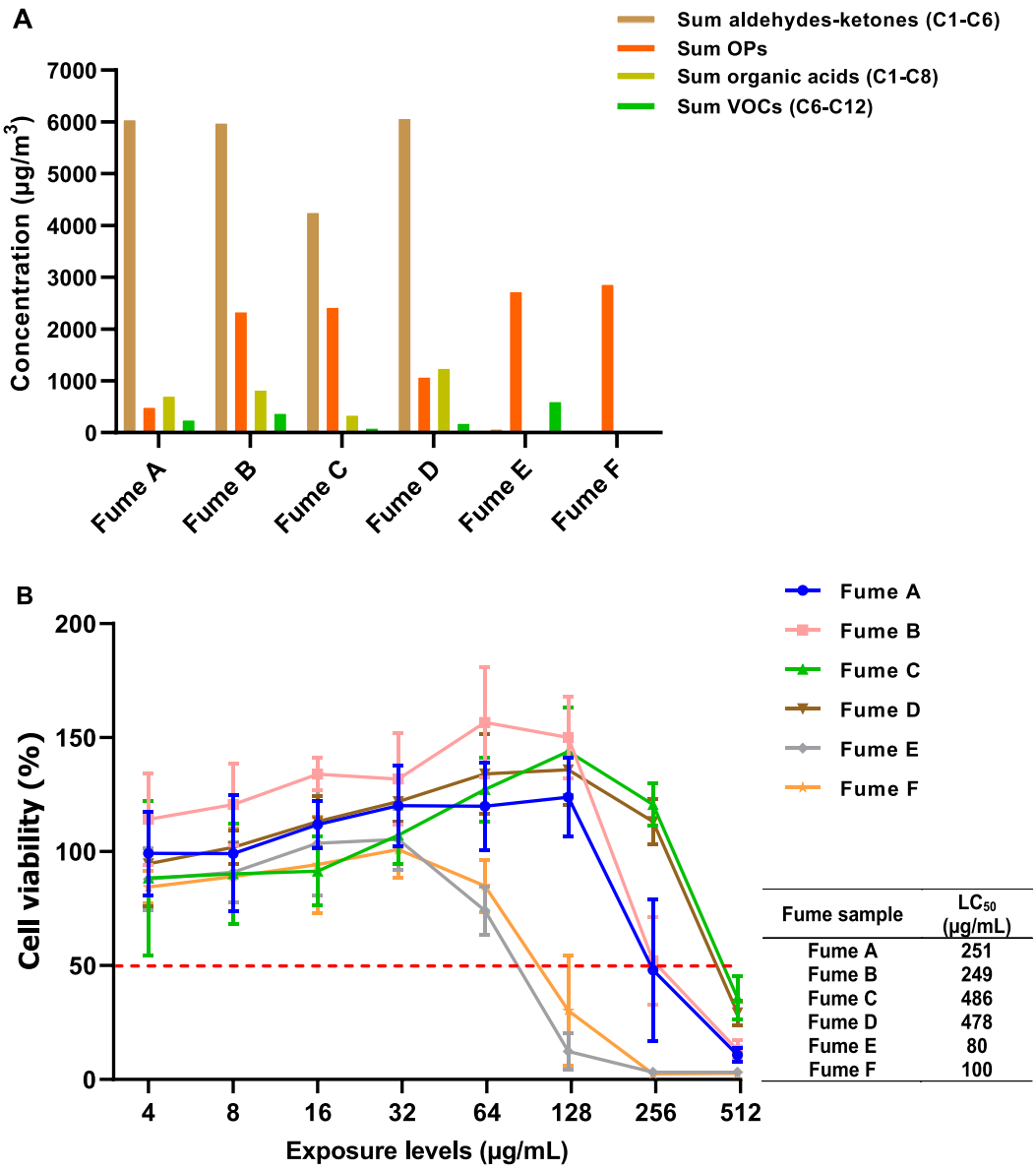

Fume sample	LC_{50} (µg/mL)
Fume A	251
Fume B	249
Fume C	486
Fume D	478
Fume E	80
Fume F	100

Fig. 2. Chemical profiles of fume samples collected on filters (A) and cell viability after submerged exposure to fume samples (B). (A) Total concentrations of aldehyde-ketones (C1- C6), OPs (32 types of OPs), organic acids (C1 – C8), and VOCs (C6 – C12) in the collected engine oil (Fume A, B, C, and D) and hydraulic fluid (Fume E and F) fumes. (B) Viability of the Calu-3 cells, determined using the WST assay, after submerged exposure to each fume sample for 24 h at 8 doses from 4 to 512 µg/mL. The red dotted line in (B) indicates 50% viability. LC_{50} represents the median lethal concentration (µg/mL) of fume samples under submerged exposure conditions. (For interpretation of the references to colour in this figure legend, the reader is referred to the web version of this article.)

Ohm × cm^2) after exposure to engine oil fumes at the tested dose-range. After exposure to hydraulic fluid fumes, a significant drop of the TEER value (lower than 500 Ohm × cm^2, $p < 0.05$) was observed in the Calu-3 cells at the highest exposure dose. However, there was no significant change in TEER values of the Calu-3 + MDM co-culture in response to hydraulic fluid fume (Fume F) exposure (Fig. 4A). After 24-hour exposure to engine oil fumes up to 100 mg/m^3, Calu-3 cells retained high cell viabilities (>80%), indicating the absence of cytotoxic effects. After exposure to hydraulic fluid fumes, viabilities of Calu-3 cells fell below 80% at >55 mg/m^3 of Fume E and 45 mg/m^3 of Fume F. In comparison to the Calu-3 monoculture, the Calu-3 + MDMs co-culture retained a high cell viability (>80%) after exposure to Fume F up to 50 mg/m^3 (Fig. 4B).

3.5. LDH release under ALI exposure conditions

In response to aircraft engine oil and hydraulic fluid fumes exposure, LDH levels on the apical side of the Calu-3 monoculture and the Calu-3 + MDM co-culture were comparable (≈ 7% of LDH_{max}) over the tested dose-ranges (Fig. 5A). In contrast, on the basolateral side, an increase in LDH release was observed at the highest dose for all of the generated fumes, with the exception of Fume A. BMD values of fume samples inducing a 20% increase in total level (apical + basolateral) of LDH release were derived from BMD analysis to rank their degree of cytotoxicity (Fig. 5A and Table 2). The BMDU of Fume A could not be determined at the tested dose-range, indicating its low cytotoxicity. Fume A was consequently not included in the rank order. According to the BMD values of hydraulic fluid fumes for LDH release (Table 2), BMDc.i. of Fume F in the Calu-3 monoculture (23–28 mg/m^3) was comparable to that in the Calu-3 + MDMs co-culture (27–34 mg/m^3). Using the Calu-3 monoculture, the BMDc.i (23–28 mg/m^3) of Fume F was lower than that of Fume E (35–45 mg/m^3). The BMDc.i of hydraulic fluid Fume E and F in the Calu-3 monoculture was much lower compared to the BMDc.i of engine oil Fume B (67–78 mg/m^3), indicating higher

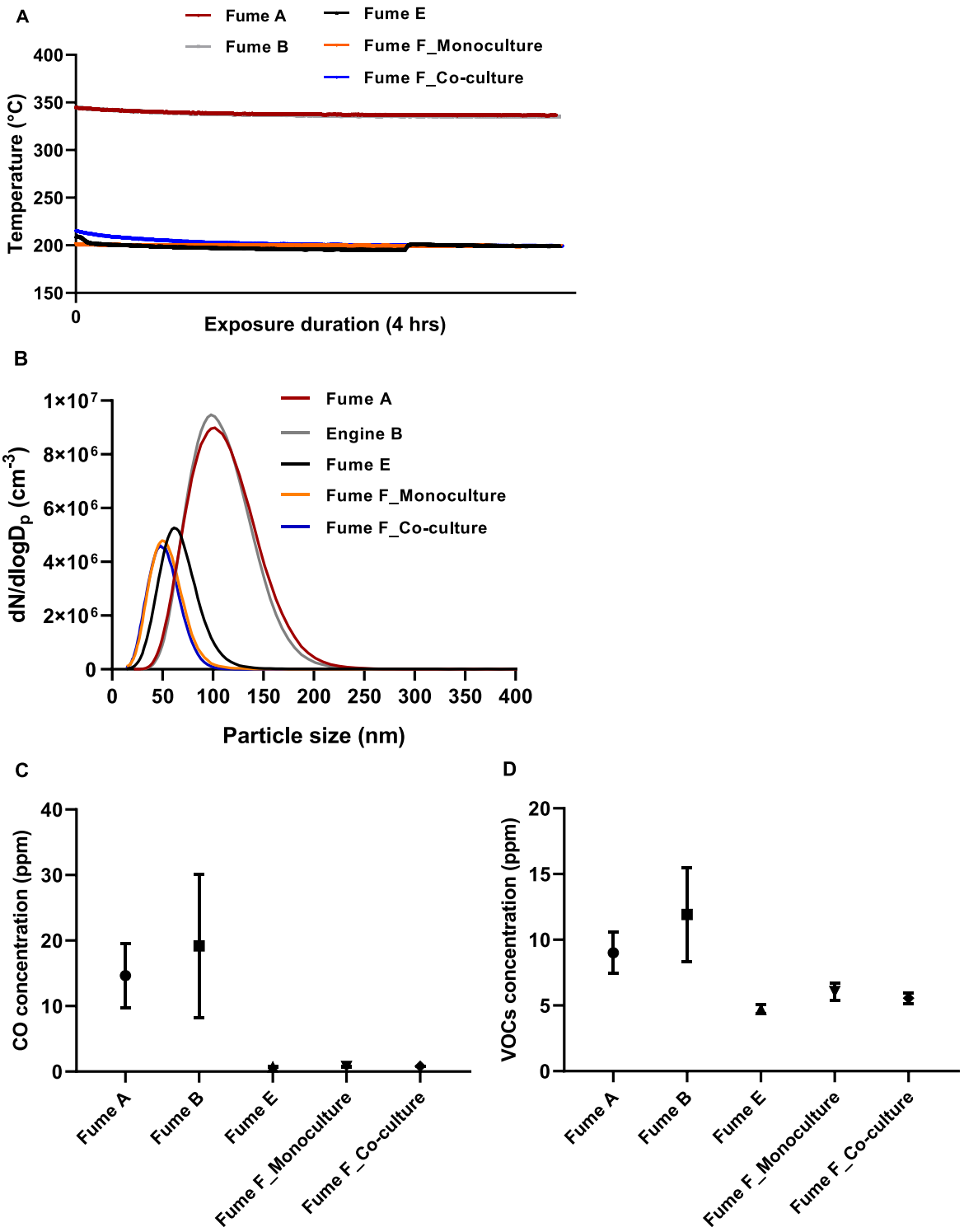

Fig. 3. Characteristics of test atmospheres during ALI exposure in the AES for 4 h. (A) Oven temperature for pyrolysis, (B) particle size distribution, (C) CO concentration, and (D) VOCs concentration of fumes generated from engine oils (Fume A and B) and hydraulic fluids (Fume E and F) during ALI exposure using the Calu-3 monoculture cell model. Fume F was also tested using the Calu-3 + MDM co-culture model.

cytotoxicity of hydraulic fluid fumes.

3.6. Inflammatory responses under ALI exposure conditions

Production of inflammatory cytokines (IL-6 and IL-8) in the apical and basolateral medium from mono- and co-culture cell models was measured after ALI exposure for 24 h (Fig. 5B and Fig. 5C). In general, levels of IL-6 and IL-8 on the apical side were much higher than on the basolateral side. On both apical and basolateral sides, an increase in IL-6 production was clearly seen for all of the generated fumes at the highest dose, with the exception of engine oil Fume A (Fig. 5B). For IL-8 production, an increase on both sides was observed only for hydraulic fluid Fume F at the highest dose using the Calu-3 monoculture model (Fig. 5C). IL-10 and TNF-α, markers for macrophages, were not detected on either side of the Calu-3 monoculture and the Calu-3 + MDM co-culture models exposed to engine oil and hydraulic fluid fumes at the

Table 1
Characteristics of test atmospheres, including the particle number concentration (PNC), geometric mean (GM) mobility diameter ± geometric standard deviation (GSD), concentrations of VOCs and CO, and mass concentration, during ALI exposure in the AES using the Calu-3 monoculture cell model. Fume F was also tested using the Calu-3 + MDM co-culture model.

Fume sample	Mean PNC (per cm^3)	Mobility diameter GM ± GSD (nm)	Mean VOCs concentration (ppm)	Mean CO concentration (ppm)	Mass concentration range (mg/m^3)
Fume A	$\sim 2.0 \times 10^8$	97 ± 3.1	9.0 ± 1.6	15 ± 4.9	0–100
Fume B	$\sim 2.3 \times 10^8$	96 ± 1.7	12 ± 3.6	20 ± 9.9	0–100
Fume E	$\sim 8.1 \times 10^7$	60 ± 9.7	4.7 ± 0.3	0.7 ± 0.1	0–55
Fume F (monoculture)	$\sim 7.8 \times 10^7$	40 ± 4.7	6.1 ± 0.7	0.7 ± 0.1	0–90
Fume F (co-culture)	$\sim 9.1 \times 10^7$	45 ± 0.7	5.6 ± 0.4	0.8 ± 0.1	0–50

tested dose-range (data not shown).

BMD values of each fume sample evoking a 20% increase of total levels (apical + basolateral) of IL-6 and IL-8 production were obtained from BMD analysis (Fig. 5B, Fig. 5C and Table 2). For aircraft engine oil fumes, the BMDU of Fume A for IL-6 production could not be determined and Fume A and B were not able to induce a BMR for IL-8 production. Therefore, Fume A was not included in the rank order of IL-6 and IL-8 production and Fume B was not included in the rank order of IL-8 production. This also indicates few pro-inflammatory effects of engine oil fumes at the tested dose-range. In comparison, a 20% increase of IL-6 and IL-8 production was identified for hydraulic fluid fumes. However, no distinctions were observed due to the substantial overlap between BMDc.i. of Fume E and Fume F (monoculture). Also, minor differences in BMDc.i. for IL-6 and IL-8 production were seen between the Calu-3 monoculture and the Calu-3 + MDMs co-culture in response to Fume F exposure.

4. Discussion

Earlier studies conducted with simulated fume events under laboratory conditions mainly focused on the composition (e.g. chemicals and particles) of aircraft engine oil and hydraulic fluid fumes (Amiri et al., 2017; Mann et al., 2014; Van Netten and Leung, 2001). Our unique combination of a Mini-BACS and an AES integrates generation of fumes from aircraft engine oils and hydraulic fluids via a bleed-air simulator under controlled conditions, deposition of the generated fumes onto the cells with a continuous airflow via the AES, and online physicochemical measurements of test atmospheres during the entire ALI exposure. This system thus provides a realistic inhalation exposure for testing toxicity of fume events *in vitro*. The toxicological data demonstrate that, for the Calu-3 mono-culture and the Calu-3 + MDM co-culture lung cell models, fumes from hydraulic fluids are more harmful than fumes derived from engine oils.

Under submerged exposure conditions, the values from the WST assay increased up to 150% of control after exposure to the generated fumes, particularly engine oil fumes, at 32–128 μg/mL for 24 h. Values from the WST assay directly correlate to the metabolic activity of the cells in the culture. It thus suggests that the cells are experiencing (oxidative) stress under exposure to engine oil fumes at 32–128 μg/mL, resulting in enhanced mitochondrial activity. Notably, the cells were exposed to oil fumes under submerged conditions by adding the fume suspension into the cell culture medium. The fume suspension consist of a mixture of particles and chemicals, which may reach the cells by sedimentation/diffusion (particles) and dissolving (chemicals), depending on their characteristics (e.g. solubility) and kinetics. The delivered dose of fumes to the cells under submerged exposure conditions consequently remains unknown. Therefore, it is difficult to compare the delivered doses of fumes under submerged conditions to the doses under ALI conditions.

Many *in vitro* studies have shown the important role of macrophages for co-culture cell models in promoting cellular responses and increasing sensitivity to particulate matter (Ji et al., 2018; Rothen-Rutishauser et al., 2007; Wottrich et al., 2004). Despite the high PNC (mean PNC $\approx 9.1 \times 10^7$) measured in Fume F, the presumed higher sensitivity of the co-culture model was not noted in our study in which we compared effects induced by Fume F in the Calu-3 + MDMs co-culture to those observed in the Calu-3 monoculture. Usually, increases in IL-10 and TNF-α production are regarded as markers for the activation of macrophages (Hoppstädter et al., 2015; Mosser and Edwards, 2008). When challenged with lipopolysaccharide (LPS) as a positive control, the Calu-3 + MDM co-culture model shows increases in IL-10 and TNF-α production and a higher sensitivity to LPS compared to the Calu-3 monoculture (He et al., 2021), indicating that MDMs in our co-culture model can be activated. However, IL-10 and TNF-α were not detected in the Calu-3 + MDM co-culture model after exposure to Fume F, suggesting that hydraulic fluid fumes did not activate macrophages under ALI exposure conditions in our study. It should be noted that during pyrolysis of hydraulic fluid at 200 °C many unburned/unreacted fluid droplets were observed in fume emission. It is therefore possible that abundant particles in hydraulic fluid fumes stick to the surface and the interior of fluid droplets, which could limit the macrophages-particles interactions when deposited onto the cells.

In this study we used BMD analysis to identify the degree of toxicity of aircraft engine oil and hydraulic fluid fumes under ALI exposure conditions. Compared to engine oil fumes, hydraulic fluid fumes had a lower BMDc.i. for LDH release and inflammatory cytokines production, indicating their higher toxicity. Different chemical profiles between engine oil and hydraulic fluid fumes may be an explanation for their different toxic properties. A number of studies have discussed the possibility of OP formation from fume events and their potential harmful effects on cabin crews and passengers (Hood, 2001; Liyasova et al., 2011; NRC, 2002; Solbu et al., 2011). Additionally, tri-n-butyl phosphate (TBP) and triphenyl phosphate (TPP), which were detected in the generated fumes (Table S2), have previously been shown to reduce cell viability (200 μM of TBP and TPP) of the lung cell lines *in vitro* and induce cytotoxicity (5 μL TBP, 20% v/v in *n*-dodecane) in lungs of *rats in vivo* (An et al., 2016; Salovsky et al., 1998). To estimate the contribution of OPs from fumes on cytotoxicity in the lung cell models under ALI exposure conditions, we studied the relationship between total OP levels of the different fumes and the mean BMD values of those fumes for LDH release derived from ALI exposures. Total OP levels showed a significant negative correlation with the BMD values for LDH release ($R^2 = 0.96$, $p < 0.05$, Figure S2A). Notably, TBP accounted for the largest fraction (>95%) of total OP level for the different fumes (Table S2). To determine the influence of other OPs on cytotoxicity, we further conducted correlation analysis for total OP levels excluding TBP, where a significant negative correlation with the BMD values still existed ($R^2 = 0.97$, $p < 0.05$, Figure S2A). Our data therefore suggest that under ALI exposure conditions higher cytotoxicity can be induced by fumes with higher total OP levels. As such, the relatively high OP level detected in hydraulic fluid fumes may explain their higher cytotoxicity under ALI exposure conditions compared to engine oil fumes. However, such significant correlations were not observed between total OP levels and the LC_{50} values of fume samples derived from submerged exposures (Figure S2B). The poor water solubility of the most abundant OP detected in fumes (TBP and TPP: log Kow > 4, (Leo and Hoekman, 1995)) may provide an

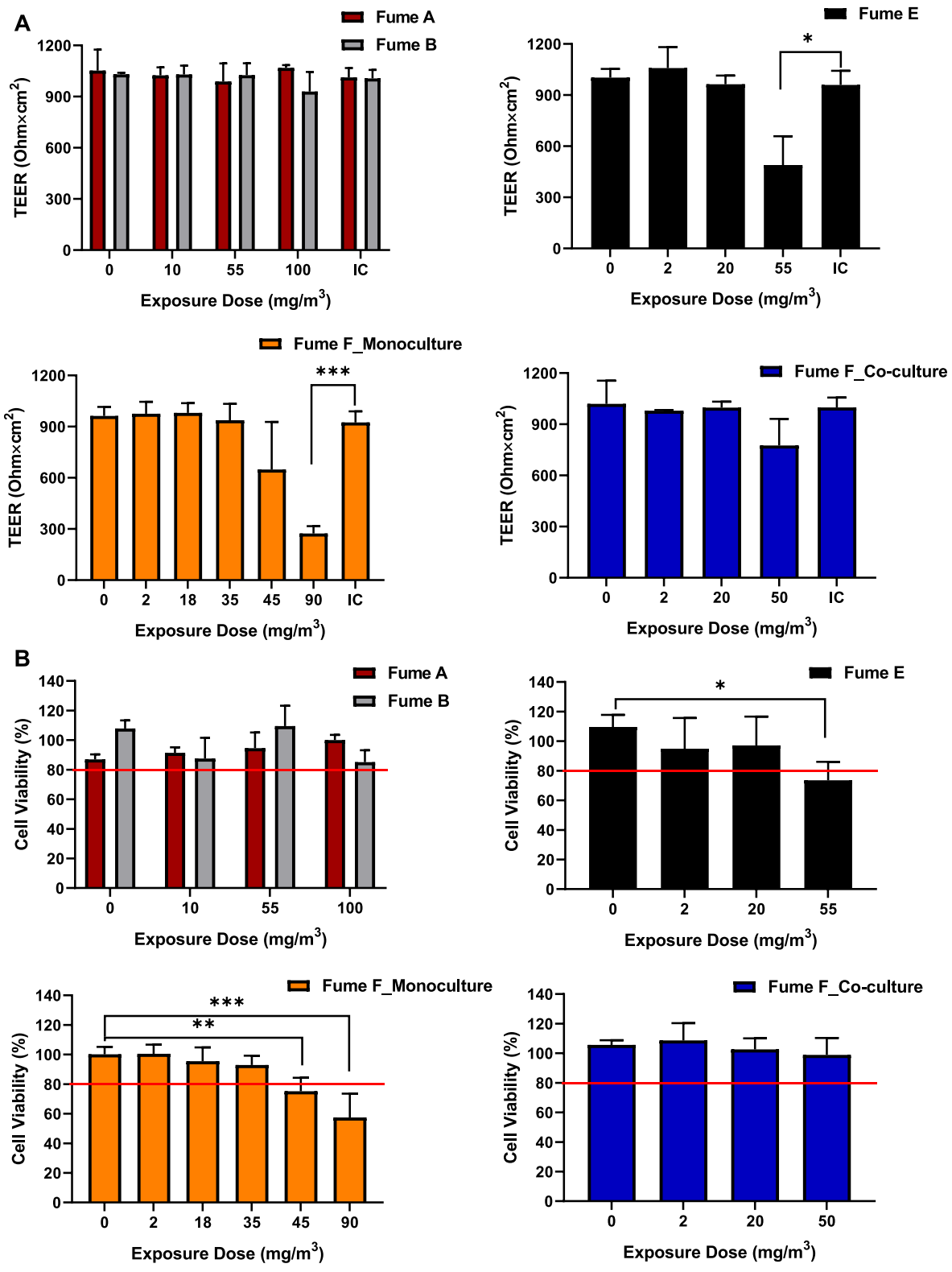

Fig. 4. TEER values (A) and viabilities (B) of the cells after ALI exposure to fumes generated from aircraft engine oils (Fume A and B) and hydraulic fluids (Fume E and F) at different doses for 24 h using the Calu-3 monoculture cell model. Fume F was also tested using the Calu-3 + MDM co-culture model. Error bars indicate the standard deviation of 3 or 6 parallel inserts with the cells. * represents $p < 0.05$, ** $p < 0.01$ and *** $p < 0.001$. The red line (B) indicates 80% viability. (For interpretation of the references to colour in this figure legend, the reader is referred to the web version of this article.)

explanation for the absence of a correlation between total OP levels and cytotoxicity under submerged conditions, as it likely prevents OPs from dissolving in the cell culture medium to a sufficient degree. In addition, smaller sized particles have larger surface area to volume ratios and higher reactivity to absorb more chemicals, thereby increasing their *in vitro* toxicity (Jonsdottir et al., 2019; Stone et al., 2017). Therefore, the smaller particle size observed in hydraulic fluid fumes (mean size ≈ 50 nm) under pyrolysis may also contribute to their higher toxicity

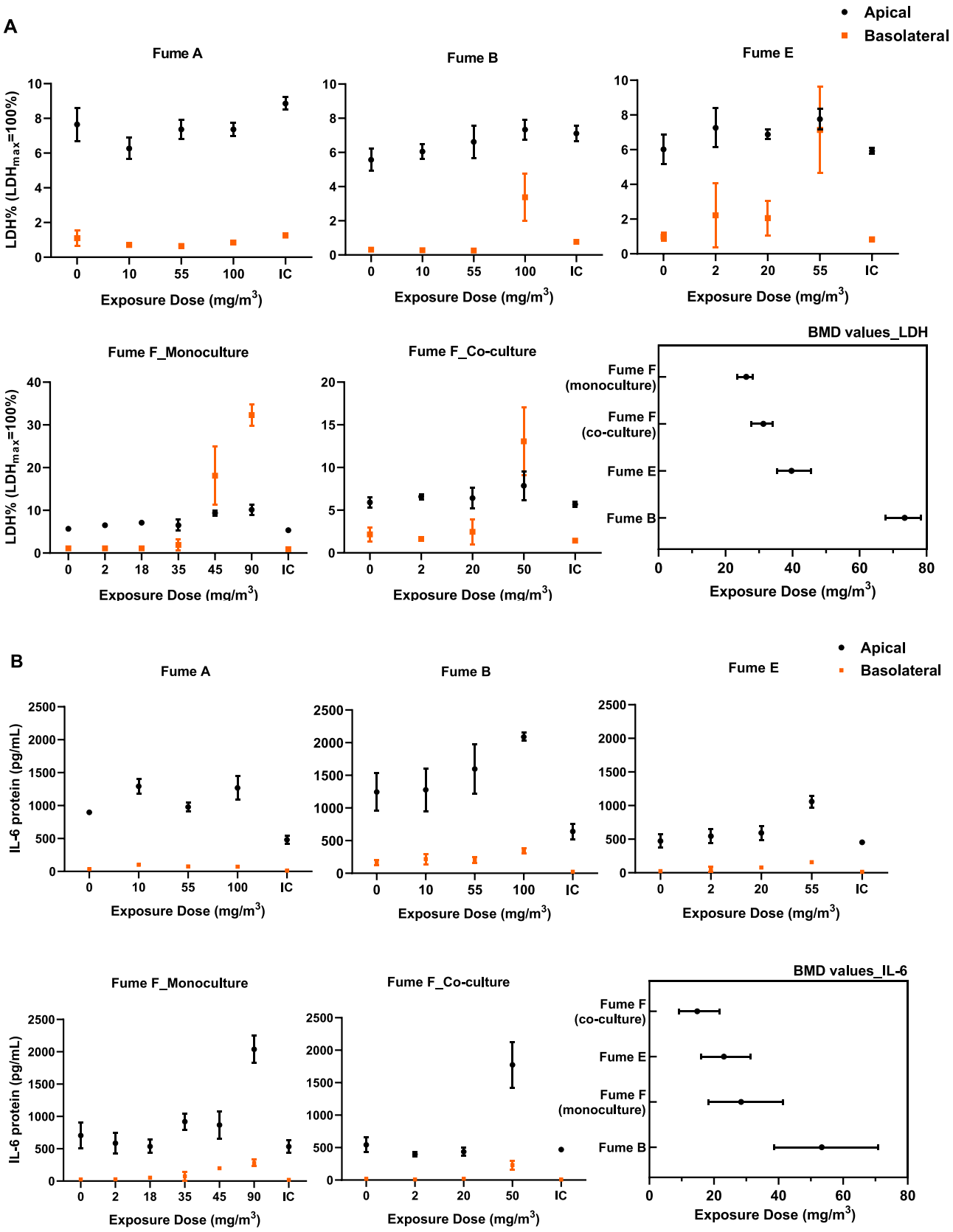

Fig. 5. Induction of cytotoxicity and inflammatory responses after ALI exposure to fumes generated from engine oils (Fume A and B) and hydraulic fluids (Fume E and F) at different doses for 24 h using the Calu-3 monoculture cell model. Fume F was also tested using the Calu-3 + MDM co-culture model. Relative LDH release (A) and production of IL-6 (B) and IL-8 (C) on the apical and basolateral sides of the inserts, combined with summary of the derived BMDc.i. and mean BMD of the different fumes for total level (apical + basolateral) of LDH release (A), IL-6 production (B) and IL-8 production (C). BMDU of Fume A could not be determined in LDH release (A) and IL-6 production (B). A 20% increase (BMR) of IL-8 production (C) could not be determined for Fume A and B. Error bars indicate the standard deviation of 3 or 6 parallel inserts with the cells. IC represents incubator control.

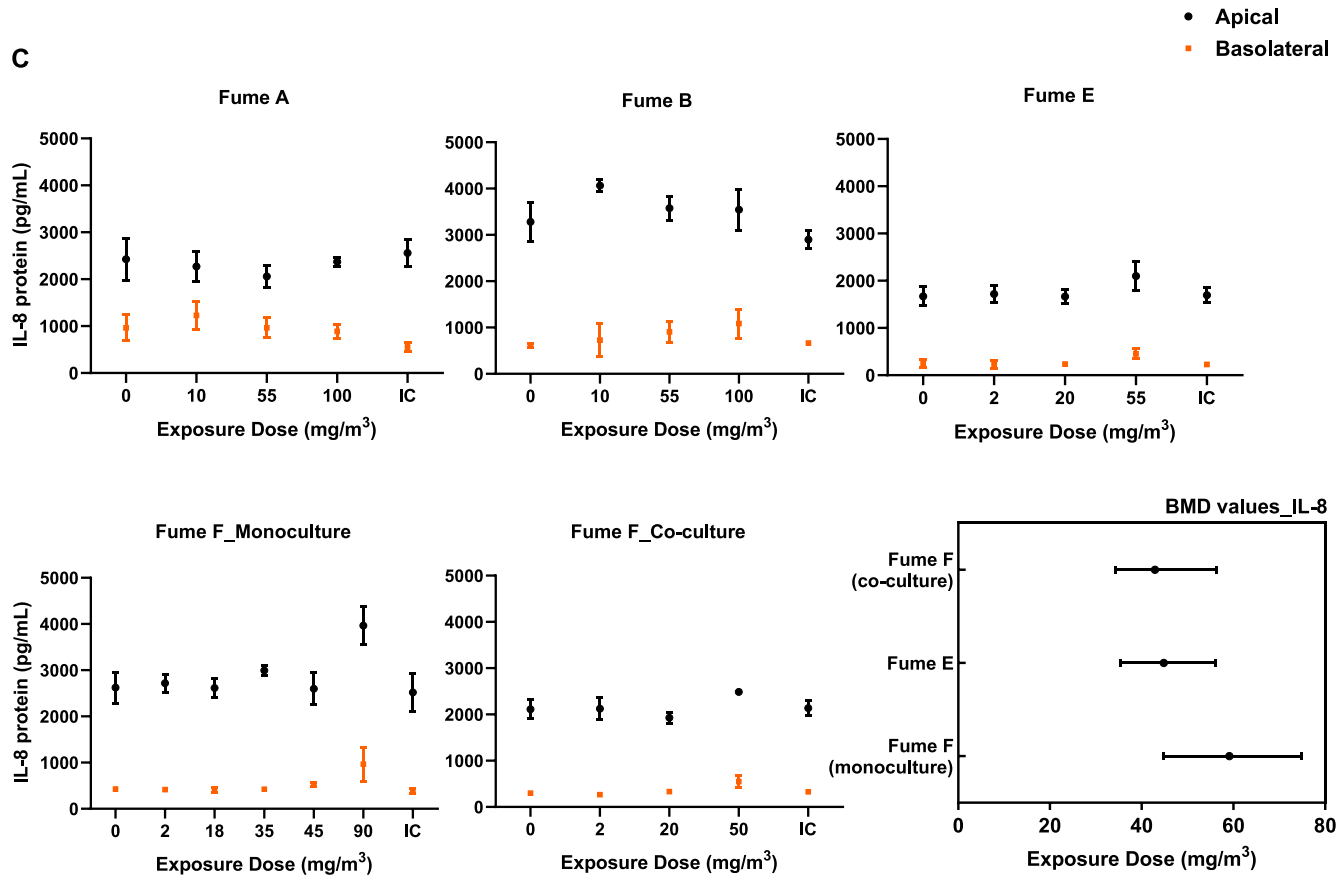

Fig. 5. (*continued*).

Table 2
Summary of the derived BMD values of the different fumes for total levels (apical + basolateral) of LDH release, IL-6 production, and IL-8 production, including the mean BMD, lower (BMDL) and upper (BMDU) limits of the confidence interval inducing a 20% BMR, after ALI exposure to fumes for 24 h using the Calu-3 monoculture cell model. Fume F was also tested with the Calu-3 + MDM co-culture model.

BMR:20%	BMD values (mg/m^3)								
	LDH			IL-6			IL-8		
	Mean	BMDL	BMDU	Mean	BMDL	BMDU	Mean	BMDL	BMDU
Fume A	140	99	–	107	64	–	–	–	–
Fume B	73	67	78	53	38	70	–	–	–
Fume E	39	35	45	23	16	31	44	35	56
Fume F (mono-culture)	26	23	28	28	18	41	59	44	74
Fume F (co-culture)	31	27	34	14	9.0	21	42	34	56

"–": could not be determined.

compared to engine oil fumes (mean size ≈ 100 nm).

Fume events are difficult to capture in real time, in part because it is not well understood under which conditions they are evoked. Consequently, there is limited knowledge on the composition and levels of inhaled fume during a fume event in an aircraft cabin. Vasak (1992) has reported that mass concentrations of fumes were respectively 1.5 mg/m^3 and 1.3 mg/m^3 in the cockpit and in the passenger cabin during a fume event. This fume level reported 20 years ago may be not the actual cabin levels under current exposure conditions, as types of aircraft engine oil have been updated and changed in the past 20 years. However, no newer data on fume/particle concentrations have been published in the open literature, to our knowledge. According to the multiple path particle dosimetry (MPPD) model analysis, the deposition efficiency of particles (10 nm < particle size < 100 nm) onto the tracheobronchial epithelium ranges from 10% to 40% (Braakhuis et al., 2014). It can thus be estimated that the inhaled level of fume into the human tracheobronchial region theoretically ranges from 0.13–0.6 mg/m^3. Although mass concentrations of engine oil (0–100 mg/m^3) and hydraulic fluid (0–90 mg/m^3) fumes during ALI exposure in our study are substantially higher, the deposition efficiency of UFPs in the AES (with the same exposure parameters used for ALI exposure to fumes) is low at around 2% for aerosolized UFPs (particle size ≈ 60 nm, data not shown). Upper estimates for exposure levels of fumes onto the cells in our study thus amount to around 2.0 mg/m^3. Using the BMD values (Table 2), we can estimate that, after adjusting for deposition efficiency (2%), the BMDL values of Fume A for LDH release (1.98 mg/m^3) and IL-6 production (1.28 mg/m^3) in the Calu-3 cells differ slightly from the realistic exposure levels of fume in the lungs (0.13–0.6 mg/m^3). For Fume B, this difference is even smaller with the BMDL for LDH release (1.34 mg/m^3) and IL-6 production (0.76 mg/m^3). For Fume E, the BMDL values for LDH release (0.70 mg/m^3), IL-6 production (0.32 mg/m^3), and IL-8 production (0.70 mg/m^3) fall within realistic exposure levels of fume

in the lungs. This also holds for the BMDL of Fume F for LDH release (0.46 mg/m^3), IL-6 production (0.36 mg/m^3), and IL-8 production (0.88 mg/m^3) using the Calu-3 monoculture model as well as for LDH release (0.54 mg/m^3), IL-6 production (0.18 mg/m^3), and IL-8 production (0.68 mg/m^3) using the Calu-3 + MDMs co-culture model. Additionally, cabin fume is a complex mixture of gases and particles, in which the gaseous part is likely also toxic to the lungs. Therefore, the main gaseous contaminants (CO and VOCs) during fume events should also be taken into consideration to comprehensively evaluate how the fume levels in test atmospheres *in vitro* relate to exposure conditions in aircraft cabins. The reported levels of CO ranged from < 1 to 9.4 ppm and VOCs ranged from below the limit of detection to ≈ 10 ppm in aircraft cabin air (Shehadi et al., 2016). It is clear that CO and VOCs levels measured in test atmospheres (CO: 0.7–20 ppm; VOCs: 4.7–12 ppm) during *in vitro* exposure substantially overlap with the realistic cabin levels. The toxicological data derived from ALI exposures in our study thus clearly reflect the potential health risks associated with fume events in aircraft cabins, particularly for hydraulic fluid fumes.

5. Conclusion

Our unique experimental "Mini-BACS + AES" setup is able to provide steady conditions to perform *in vitro* exposure under ALI conditions to aircraft engine oil and hydraulic fluid fumes, generated at respectively 350 °C and 200 °C. Exposure of the Calu-3 monoculture and Calu-3 + MDM co-culture lung cell models to high levels of aircraft engine oil and hydraulic fluid fumes under ALI conditions can reduce TEER and viabilities of the cells, induce cytotoxicity, and increase production of pro-inflammatory cytokines. Hydraulic fluid fumes are more toxic than engine oil fumes on the mass concentration of fume basis, which may be related to higher abundance of OPs and smaller particle size of hydraulic fluid fumes. Our toxicological data clearly reflect the potential health risks during fume events in aircraft cabins.

CRediT authorship contribution statement

Rui-Wen He: Conceptualization, Methodology, Investigation, Data curation, Formal analysis, Writing - original draft. **Marc M.G. Houtzager:** Conceptualization, Methodology, Data curation, Writing - review & editing. **W.P. Jongeneel:** Conceptualization, Project administration, Writing - review & editing. **Remco H.S. Westerink:** Conceptualization, Writing - review & editing. **Flemming R. Cassee:** Conceptualization, Supervision, Writing - review & editing.

Declaration of Competing Interest

The authors declare that they have no known competing financial interests or personal relationships that could have appeared to influence the work reported in this paper.

Acknowledgements

Part of this work was performed under the service contract MOVE/BE/SER/2016-363/SI2.748114 – "Investigation of the quality level of the air inside the cabin of large transport aeroplanes and its health implication" funded by the Directorate-General for Mobility and Transport (DG MOVE) of the European Commission. We thank Rob Vree Egberts, Paul H.B. Fokkens and Eric R. Gremmer from the National Institute for Public Health and the Environment (RIVM) for their valuable assistance with the "Mini-BACS + AES" setup and *in vitro* exposure. The support provided by China Scholarship Council (CSC) during the PhD period of Rui-Wen He in Utrecht University-Institute for Risk Assessment Studies is also acknowledged.

Appendix A. Supplementary data

Supplementary data to this article can be found online at https://doi.org/10.1016/j.envint.2021.106718.

References

Abou-Donia, M.B., Abou-Donia, M.M., ElMasry, E.M., Monro, J.A., Mulder, M.F., 2013. Autoantibodies to nervous system-specific proteins are elevated in sera of flight crew members: biomarkers for nervous system injury. J. Toxicol. Environ. Health, Part A 76, 363–380.
Amiri, S.N., Jones, B., Mohan, K.R., Weisel, C.P., Mann, G., Roth, J., 2017. Study of aldehydes, carbon monoxide, and particulate contaminants generated in bleed-air simulator. J. Aircraft 54, 1364–1374.
An, J., Hu, J., Shang, Y., Zhong, Y., Zhang, X., Yu, Z., 2016. The cytotoxicity of organophosphate flame retardants on Hep G2, A549 and Caco-2 cells. J. Environ. Sci. Health, Part A 51, 980–988.
Braakhuis, H.M., Park, M.V., Gosens, I., De Jong, W.H., Cassee, F.R., 2014. Physicochemical characteristics of nanomaterials that affect pulmonary inflammation. Part. Fibre Toxicol. 11, 18.
Brown, T.P., Shuker, L.K., Rushton, L., Warren, F., Stevens, J., 2001. The possible effects on health, comfort and safety of aircraft cabin environments. J. Royal Soc. Promotion Health 121, 177–184.
Denola, G., Hanhela, P., Mazurek, W., 2011. Determination of tricresyl phosphate air contamination in aircraft. Ann. Occup. Hyg. 55, 710–722.
EFSA, 2009. Guidance of the Scientific Committee on Use of the benchmark dose approach in risk assessment. EFSA J. 7, 1150.
He, R.-W., Braakhuis, H.M., Vandebriel, R.J., Staal, Y.C.M., Gremmer, E.R., Fokkens, P.H. B., Kemp, C., Vermeulen, J., Westerink, R.H.S., Cassee, F.R., 2021. Optimization of an air-liquid interface in vitro cell co-culture model to estimate the hazard of aerosol exposures. J. Aerosol Sci. 153, 105703.
He, R.-W., Gerlofs-Nijland, M.E., Boere, J., Fokkens, P., Leseman, D., Janssen, N.A., Cassee, F.R., 2020. Comparative toxicity of ultrafine particles around a major airport in human bronchial epithelial (Calu-3) cell model at the air–liquid interface. Toxicology in Vitro 104950.
He, R.-W., Shirmohammadi, F., Gerlofs-Nijland, M.E., Sioutas, C., Cassee, F.R., 2018. Pro-inflammatory responses to PM0. 25 from airport and urban traffic emissions. Sci. Total Environ. 640, 997–1003.
Hood, E., 2001. OPs cause bad trips? Environmental health perspectives. 109, A156-A156.
Hoppstädter, J., Seif, M., Dembek, A., Cavelius, C., Huwer, H., Kraegeloh, A., Kiemer, A. K., 2015. M2 polarization enhances silica nanoparticle uptake by macrophages. Front. Pharmacol. 6, 55.
Howard, C., Johnson, D., Morton, J., Michaelis, S., Supplee, D., Burdon, J., 2018. Is a cumulative exposure to a background aerosol of nanoparticles part of the causal mechanism of aerotoxic syndrome. J. Nanomed. Nanosci.: JNAN-139.
Hu, G., Christman, J.W., 2019. Alveolar macrophages in lung inflammation and resolution. Front. Immunol. 10, 2275.
Ji, J., Upadhyay, S., Xiong, X., Malmlöf, M., Sandström, T., Gerde, P., Palmberg, L., 2018. Multi-cellular human bronchial models exposed to diesel exhaust particles: assessment of inflammation, oxidative stress and macrophage polarization. Part. Fibre Toxicol. 15, 19.
Jonsdottir, H.R., Delaval, M., Leni, Z., Keller, A., Brem, B.T., Siegerist, F., Schönenberger, D., Durdina, L., Elser, M., Burtscher, H., 2019. Non-volatile particle emissions from aircraft turbine engines at ground-idle induce oxidative stress in bronchial cells. Commun. Biol. 2, 1–11.
Leo, A., Hoekman, D., 1995. Exploring QSAR. American Chemical Society.
Liyasova, M., Li, B., Schopfer, L.M., Nachon, F., Masson, P., Furlong, C.E., Lockridge, O., 2011. Exposure to tri-o-cresyl phosphate detected in jet airplane passengers. Toxicol. Appl. Pharmacol. 256, 337–347.
Mann, G.W., Eckels, S.J., Jones, B.W., 2014. Analysis of particulate size distribution and concentrations from simulated jet engine bleed air incidents. HVAC&R Research. 20, 780–789.
Michaelis, S., 2011. Contaminated aircraft cabin air. J. Biol. Phys. Chem. 11, 132–145.
Michaelis, S., 2016. Oil bearing seals and aircraft cabin air contamination. Sealing Technol. 2016, 7–10.
Michaelis, S., Burdon, J., Howard, C.V., Organization, W.H., 2017. Aerotoxic syndrome: a new occupational disease? Public Health Panorama 3, 198–211.
Mosser, D.M., Edwards, J.P., 2008. Exploring the full spectrum of macrophage activation. Nat. Rev. Immunol. 8, 958–969.
NRC, 2002. The airliner cabin environment and the health of passengers and crew. National Academies Press. https://doi.org/10.17226/10238.
OHRCA, 2014. http://www.ohrca.org/wpcontent/uploads/2014/08/finalreport.pdf.
Ramsden, J.J., 2012. Contaminated aircraft cabin air: aspects of causation and acceptable risk. J. Biol. Phys. Chem. 12, 56–68.
Reneman, L., Schagen, S.B., Mulder, M., Mutsaerts, H.J., Hageman, G., de Ruiter, M.B., 2016. Cognitive impairment and associated loss in brain white microstructure in aircrew members exposed to engine oil fumes. Brain Imaging Behav. 10, 437–444.
Rothen-Rutishauser, B., Mühlfeld, C., Blank, F., Musso, C., Gehr, P., 2007. Translocation of particles and inflammatory responses after exposure to fine particles and nanoparticles in an epithelial airway model. Part. Fibre Toxicol. 4, 1–9.
Salovsky, P., Shopova, V., Dancheva, V., 1998. Antioxidant defense mechanisms in the lung toxicity of tri-n-butyl phosphate. Am. J. Ind. Med. 33, 11–15.

Shehadi, M., Jones, B., Hosni, M., 2016. Characterization of the frequency and nature of bleed air contamination events in commercial aircraft. Indoor Air 26, 478–488.
Solbu, K., Daae, H.L., Olsen, R., Thorud, S., Ellingsen, D.G., Lindgren, T., Bakke, B., Lundanes, E., Molander, P., 2011. Organophosphates in aircraft cabin and cockpit air—method development and measurements of contaminants. J. Environ. Monit. 13, 1393–1403.
Stone, V., Miller, M.R., Clift, M.J., Elder, A., Mills, N.L., Møller, P., Schins, R.P., Vogel, U., Kreyling, W.G., Alstrup Jensen, K., 2017. Nanomaterials versus ambient ultrafine particles: an opportunity to exchange toxicology knowledge. Environ. Health Perspect. 125, 106002.
Van Netten, C., 2005. Aircraft air quality incidents, symptoms, exposures and possible solutions. Air Quality in Airplane Cabins and Similar Enclosed Spaces 193–210.
Van Netten, C., Leung, V., 2001. Hydraulic fluids and jet engine oil: pyrolysis and aircraft air quality. Arch. Environ.: Int. J. 56, 181–186.
Vasak, V., 1992. Cabin Air Contamination in BAe 146 in EastWest Airlines. Industrial Hygiene and Environmental Service Laboratories, St Ives.
Winder, C., Balouet, J.-C., 2002. The toxicity of commercial jet oils. Environ. Res. 89, 146–164.
Winder, C., Michaelis, S., 2005. Crew effects from toxic exposures on aircraft. Air Quality in Airplane Cabins and Similar Enclosed Spaces. 229–248.
Wottrich, R., Diabaté, S., Krug, H.F., 2004. Biological effects of ultrafine model particles in human macrophages and epithelial cells in mono-and co-culture. Int. J. Hyg. Environ. Health 207, 353–361.